Registration and Fusion of CT and MRI of the Temporal Bone

Soenke Heinrich Bartling, MD,* Kersten Peldschus, MD,* Thomas Rodt, MD,† Florian Kral, MD,‡ Herbert Matthies, PhD,§ Ron Kikinis, MD,‡ and Hartmut Becker, MD*

Objective: To present and evaluate a registration method to fuse complementary information of CT and MRI of the temporal bone.

Methods: CT and MRI of the temporal bone of 26 patients were independently registered 4 times. A manual, iterative, intrinsic, rigid, and retrospective registration method was used. Mean CRE_m (consistency registration error) was calculated as a reproducibility measurement.

Results: CRE_m was 0.6 mm (95% CI = 0.52–0.68 mm). T-test revealed no difference between pathologic and normal cases (t[102] = −1.71; P = 0.09). Time needed: 13 minutes. In the registered and fused datasets, important bony surgical landmarks (eg, facial nerve canal, inner ear) could be assessed in 3 dimensions relatively to tumor tissue (eg, acoustic schwannoma). Fluid distribution within partially obliterated cochleae could be assigned to either scalae.

Conclusion: An accurate, reproducible registration and fusion method that improves tumor surgery and cochlea implantation planning with only minor changes to the clinical workflow was presented and described. We suggest this method in selected cases.

Key Words: CT, MRI, registration, temporal bone, cochlea implantation, myotonic dystrophy

CT and MRI of the temporal bone provide complementary information about temporal bone structures and pathologies. CT allows imaging of bony structures, whereas MRI enables imaging of soft tissue structures.

It has been shown in previous studies that image registration and fusion gains a significant improvement over conventional images in depicting the relationship between bone and soft tissue.[1,2] We assume that temporal bone imaging could also benefit from registration and fusion. However, image fusion of the temporal bone has not been described for clinical diagnostic purpose so far.[3]

An accurate image registration and fusion could be especially useful in the temporal bone, because here, small soft tissue structures are embedded in the surrounding bone.[4] For example, to assess the facial nerve along its entire course, one has to switch from the direct MR imaging of the nerve in the internal auditory canal (IAC) to the indirect CT imaging of its bony canal, aligning the images mentally for this transition. The same problem occurs when other structures such as the inner ear and IAC and their bony delineation need to be aligned. Furthermore, a mental integration of both modalities is especially difficult in CT and MRI of the temporal bone, because often in clinical routine different scan planes are used for each modality (Fig. 1).

The main goals of this study were to present and evaluate a registration method of CT and MRI that could be done retrospectively in clinical routine and to describe the potential benefits for diagnosing and surgical planning in selected temporal bone pathologies.

MATERIALS AND METHODS

Data Acquisition

Twenty-six patients (16 female, 10 male, mean age 25.04 years, SD 24.8 years, range 1–71 years) who routinely underwent CT and MRI examination of the temporal bone were retrospectively identified. Helical CT studies were acquired using a 4-slice CT scanner (Lightspeed Qx/i, GE Healthcare, Milwaukee, WI) applying a low-dose protocol (140 kV, 80 mA, 1.25-mm collimation, pitch = 3).[5] Images were reconstructed using a 180° LI bone algorithm with a field of view (FOV) of 16 cm and a reconstruction matrix of 512 × 512 pixels, with an interval of 0.6 mm, resulting in voxel size of 0.31 mm × 0.31 mm × 0.6 mm. The MRI studies were performed using 2 1.5-Tesla MRI systems (Signa Horizon and NV/I; GE Healthcare, Milwaukee, WI).[6] As part of the routine protocol, all patients underwent high-resolution imaging of the
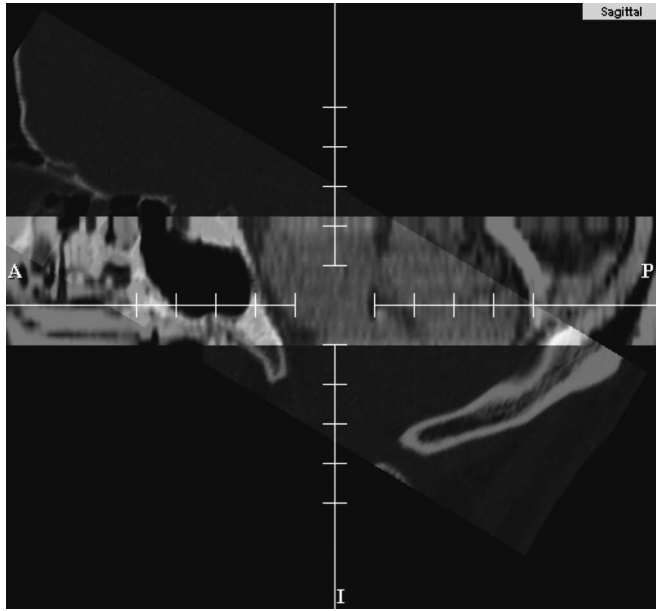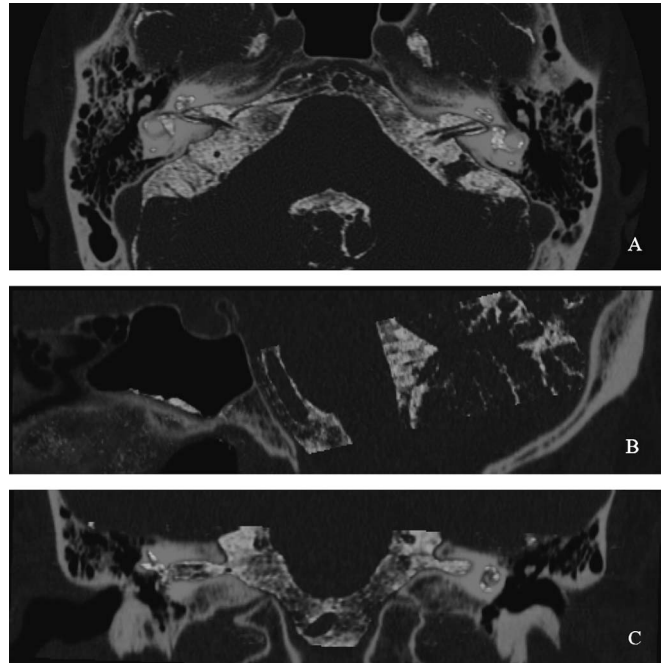
FIGURE 1. In clinical routine, the CT scan plane is tilted compared with the MRI scan plane to minimize radiation on the eye lens. This hinders a mental integration of both modalities.

FIGURE 2. Co-registration of CT and MRI scan of the temporal bone and adjacent skull base. The iterative, manual registration method requires visual assessment in 3 orthogonal planes: Axial plane at the level of the internal acoustic meatus (A), sagittal plane shows the sella turcica (B), and coronal plane at the level of the internal acoustic meatus (C).

inner ear applying a T2-weighted 3-dimensional fast spin echo (3D-FSE; TR/TE/NEX, 4400 milliseconds/120 milliseconds/l) sequence in 10 patients and a T2-weighted 3-dimensional fast imaging employing steady state acquisition (3D-FIESTA; TR/TE/NEX 10.5 milliseconds/4.9ms/1) sequence in the other 16 patients using a standard headcoil. Acquisition matrix was 512×512 over a FOV of 20–28 cm with section thickness of 0.7–1.0 mm, resulting in a voxel sizes of 0.39–0.54 mm $\times$ 0.39–0.54 mm $\times$ 0.7–1.0 mm. Indications for the examinations were preoperative evaluation of cochlea implant candidates and assessment of tumorous involvement of the temporal bone. Patients were grouped according to the diagnostic reporting. In 13 patients, CT and MRI revealed no abnormal pathologic findings. Thirteen patients presented with inner ear malformations, obliterations of the cochlea and labyrinth, or tumorous involvement.

Registration and Image Processing

An experimental software package (3D-Slicer, Surgical Planning Laboratory, Brigham and Women's Hospital, Harvard Medical School, Boston, MA, www.slicer.org)[7] was used for image co-registration and 3-D data visualization. The program provided a framework to co-register 2 data sets in 3 different orthogonal orientations and with arbitrary levels of transparent overlays (Fig. 2). Semitransparent MRI images were registered to the CT images by moving and rotating the MRI relatively to the CT. The matching of corresponding structures in both data sets was assessed and the transformation was gradually refined to optimize structure overlap. The end point was user satisfaction.[8] Four independent co-registrations were carried out by 2 operators (K. P., F. K.) for each patient. 3D models of the inner ear and adjacent structures were generated in selected cases. Therefore, anatomic

structures and tumors were isolated from the image volume by a threshold and/or manual segmentation. A color-coded surface-rendering algorithm was used for 3-D visualization. Images were generated showing the 3D models and 2D/3D correlated projections.

Data Analysis

A mathematical software package (Matlab 6.1, The MathWorks, Inc., Natick, MA) was used to determine the co-registration reproducibility. The consistency registration error (CRE) was calculated for each patient by comparing the 4 independent registration matrices with their mean registration matrix that were assumed to be the standard of reference.[9] To transform the resulting CRE-matrix into a linear dimension, it was applied to 500 voxels stochastically spread in a region covering both pyramids of the temporal bone. Subsequently the root mean square displacement of all voxels was calculated to average the results over this region of interest. The CRE values were assessed for patients with pathologic findings (CRE_p) and without pathologic findings (CRE_n), respectively, and followed by a Student's t test to compare the results of both groups. Finally, the mean CRE_m was calculated for all 26 cases.

Furthermore, the upper limit of the 95% confidence interval (CI) of CRE_m was compared with reported measurements of the diameter of the IAC[10] and the vestibular and tympanic scalae.[11] In the latter, dimensions were given as mean area values. The average diameter was calculated in

assumption of a circular area. Therefore, the average diameter is interpreted as a mean value of the width of each structure.

The fused images were evaluated regarding their ability to delineate the relationships between bony and soft tissue structures of the temporal bone.

RESULTS

CT and MRI data sets could be co-registered in all of the 26 cases. We found that an effective approach for iterative manual co-registration was to start with the alignment of both IAC in the axial and coronal slices. The MRI images were then rotated on sagittal slices around the axis formed by both IAC to align the frontal lobes and the cerebellum with the anterior and posterior cranial fossa. The final alignment was achieved using inner ear landmarks such as parts of the cochlea, vestibule, and semicircular canals. The average time needed for manual co-registration was 13 minutes (range 8–19 minutes).

Assessment of the CRE resulted in the following values: In the group of patients with normal findings, CRE_n was 0.54 mm (95% CI = 0.45–0.62 mm). For the group of patients with pathologic, findings a CRE_p of 0.67 mm (95% CI = 0.53–0.80 mm) could be determined. Comparison of the mean of the 2 patient groups revealed no statistically significant difference (t[102] = −1.71; P = 0.09). The overall mean value for CRE_m (n = 26) was 0.60 mm (95% CI = 0.52–0.68 mm) within a range from 0.24 mm to 1.67 mm.

Comparison of the upper limit of the 95% CI of CRE_m to the dimensions of the width of the vestibular scala and the tympanic scala and the IAC resulted in the following ratios: 46.8% and 42.2% of the width of the vestibular scala and tympanic scala; 14.1% of the axial diameter of the fundus of the internal acoustic meatus.

The nerves could be clearly localized in the bony IAC. The different branches of the vestibulocochlear nerve could be assessed in the lower story of the IAC and could be followed to the cochlea and the vestibule (Fig. 3). The course of the facial nerve could be followed from the brain stem to the parotid gland. A seamless transition from its direct MRI in the IAC to the indirect CT imaging in its bony canal was displayed (Fig. 3).

Tumors in the IAC could be localized relative to the bone. Depth of tumor-growth could be clearly assessed in the IAC (Fig. 4).

In the fused images, the distribution of the fluid signal within the inner ear could be clearly assessed relatively to the bony labyrinth. Also, in cases without total obliteration of the cochlea, the accuracy of the registration process allowed a decision about whether the attenuated fluid stemmed from the scala vestibuli or scala tympani (Fig. 5). Furthermore, the fluid distribution within the cochlea could also be vividly demonstrated using 3D renderings of the fused datasets (Fig. 5D).

DISCUSSION

Registration Method

In respect to the proposed practical use, image processing has to be evaluated for accuracy. Medical image co-registration is rated according to a gold standard and the reproducibility of the specific algorithm that is used. Applying
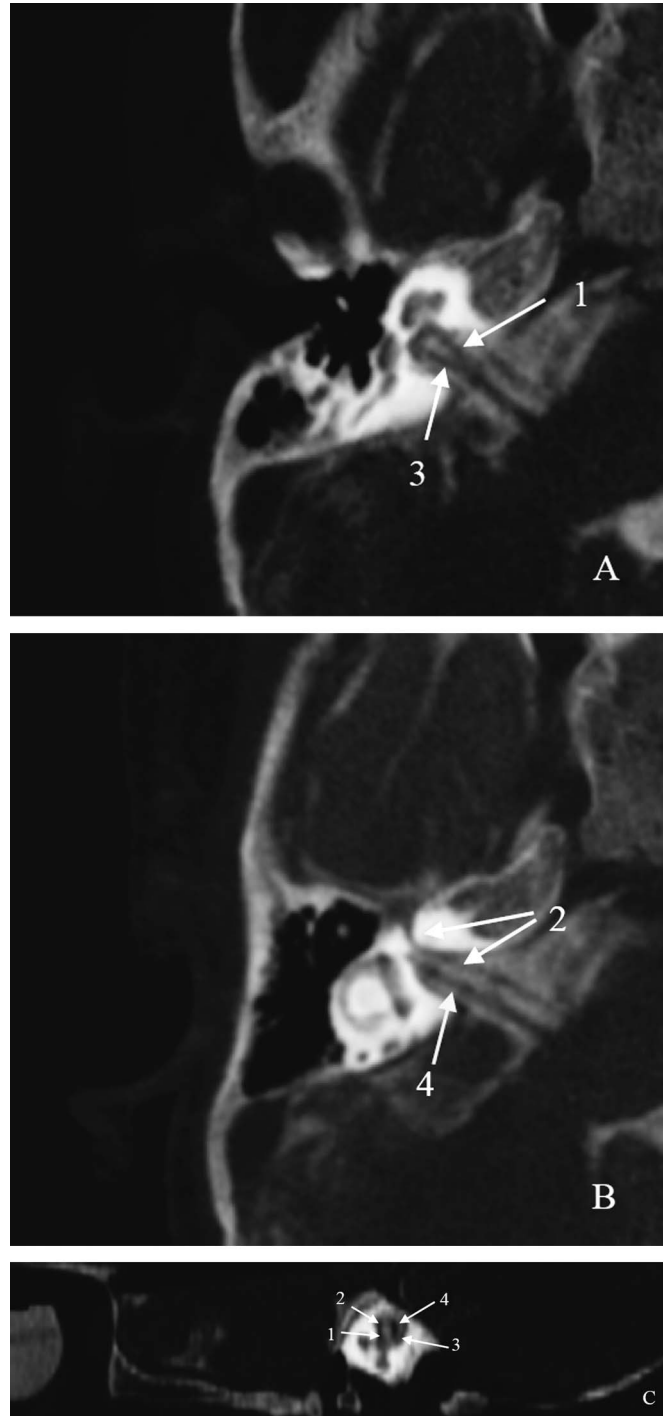
FIGURE 3. Reformatted fused Images showing the content of the IAC. The up-branching of the vestibulocochlear nerve in its cochlear (1), superior vestibular (3), and inferior vestibular (4) branch can be found in the lower story (A) and upper story (B) of the IAC. The branches can be followed to the cochlea and the vestibule. The facial nerve (2) can be seamlessly followed through the IAC into its bony canal (B). On sagittal reformations, all 4 structures can be assessed relatively to the surrounding bone (C).
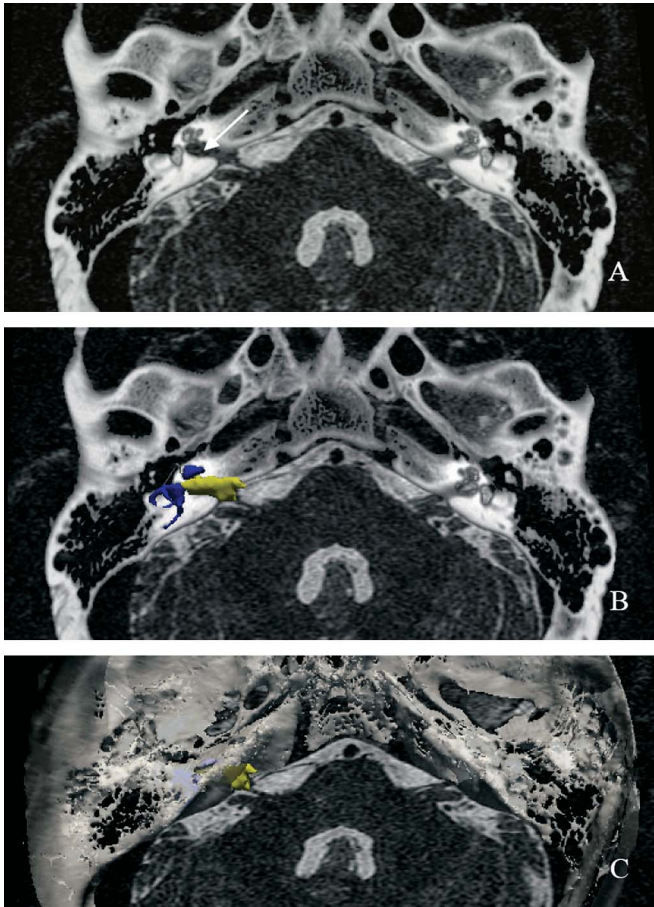
FIGURE 4. Acoustic schwannoma in the right internal auditory canal (arrow) in registered and fused CT and MRI of the temporal bone. For surgical planning, the MRI-given tumor (yellow) and critical CT-given surgical landmarks such as the labyrinth (blue) and the facial nerve canal (gray) (B) as well as the bony skull base (white) can be displayed together (C).

fiducial markers as a gold standard was not applicable in our retrospective study. Therefore, we were not able to absolutely quantify co-registration accuracy by quantifying the Target Registration Error (TRE).[12] However, the determination of the reproducibility by consistency measurements of 4 independent registrations revealed accurate and consistent results with a mean error of 0.6 mm. This value is close to the limitation of visual assessment that has already been described as highly sensitive to detect errors in image alignment greater than 0.2 mm.[13] Furthermore, our CRE is about the edge size of 1 voxel of either modality, which is also consistent with earlier studies that have found manual registration accuracy (TRE) of CT and MRI within the order of 1 voxel.[8,14]

The evaluation of this error compared with distinct inner ear dimensions revealed percentages less than 50% for all structures. Therefore, we rated the result as a success for registration that allows reproducible registration of temporal bone structures of clinical interest.

Results revealed no statistically significant difference between patients with and without pathologic findings regard-

ing the registration reproducibility. However, in patients having severe pathologic changes in the temporal bone anatomy, especially affecting the structures that were used for the fine alignment, the registration process was more challenging and more time-consuming.

The extensive range of the assessed registration error could be explained by user and case dependence as well as variations in MRI parameters. Due to the departmental structure, patients underwent either a 3D-FSE or 3D FIESTA sequence with different spatial parameters. Consequently, this led to an influence of the calculation of the registration error, taking into account the voxel size for the linear transformation of CRE in each case.

Other registration methods vary regarding their reproducibility, accuracy, user dependence, and effort necessary. We believe that the presented method is the best trade-off between effort, necessary changes to the clinical workflow, diagnostic benefit, and current feasibility. Other methods as discussed in the next paragraph would mean either big changes to the clinical workflow or are currently not described for the temporal bone.

Most exact gold standard methods need extrinsic fiducial markers that need to be placed before scanning.[9] Therefore, one would need to know beforehand that a registration and fusion are beneficial in a given case. Placing registration markers on every scanned patient is not practicable since registration does not need to be performed in obvious or normal cases. Furthermore, the decision to have a second modality scan is often a consequence of earlier studies.

The aim of automated registration methods is to present a user-independent, fast, and reproducible registration method. An automated, user-independent algorithm that produces highly reliable and accurate registration results comparable with manual or marker-based registration methods is not yet described. During the planning phase of our study, an automated registration method based on mutual information that is implemented in the 3D Slicer software was preliminarily tested. It registers images according to some sort of similarity in the image intensities.[15] While the algorithm resulted in sufficient alignment of CT and MRI of the whole head,[15] it did not result in sufficient alignment of normal temporal bone scans. That might be due to the lack of similar image features in the isolated scanned temporal bone: The MRI is more or less an exact inversion of the CT, eg, the CT of the labyrinth is low in signal, while the MRI of the labyrinth is high in signal. Also, other research has shown that automated registration algorithms can indeed result in useful registrations between CT and MRI, but regardless what algorithm used the result should still be visually inspected against big, random errors.[16] Despite the fact that these examinations were performed on head studies, it is likely that the same would hold true for temporal bone imaging. Another problem is that automated registration approaches relying on certain features of the datasets might be more problematic in pathologic cases than in cases presenting normal anatomic conditions, while the proposed usefulness of the registration and fusion applies particularly to pathologic cases. Other, more advanced algorithms or algorithms based on other image features might be more successful in the future for registering CT and MRI of the
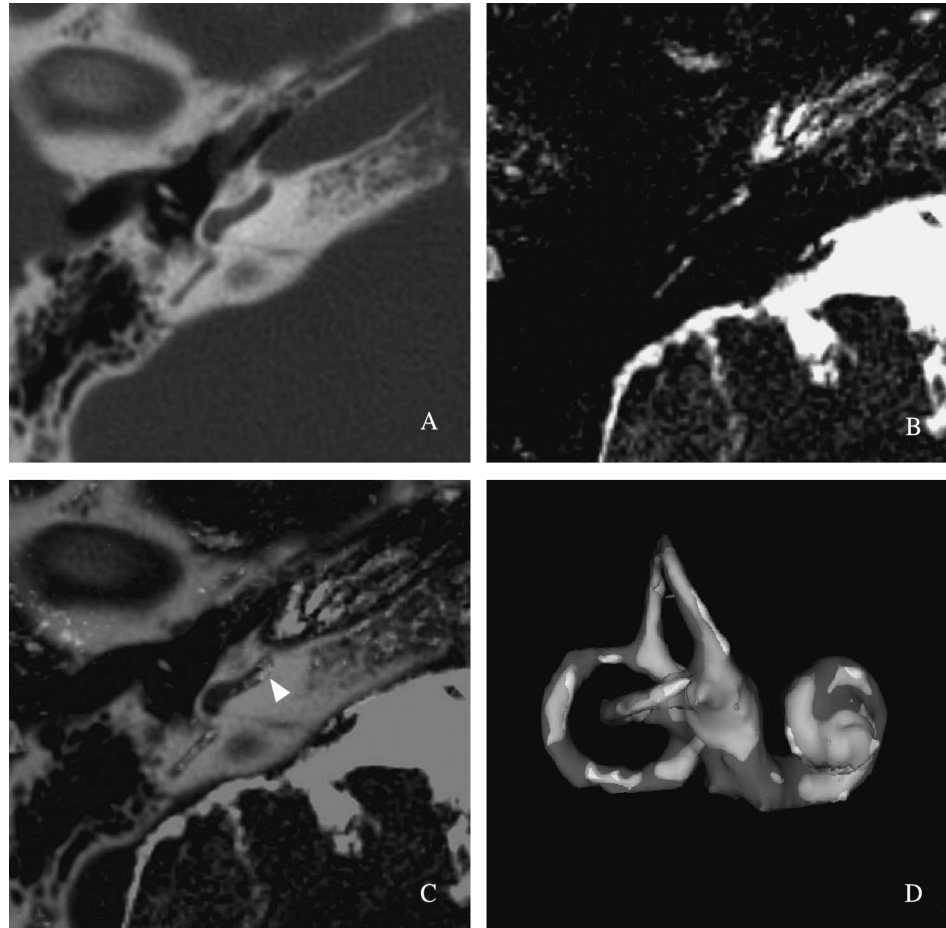
FIGURE 5. Obliterations of the labyrinth in a cochlea implant candidate. The CT axial plane on the level of cochlea basal turn reveals no abnormality (A). Corresponding MRI axial plane at the same level showing some irregularly distributed fluid signal somewhere in the cochlea. In co-registered CT and MRI, the remaining fluid signal (arrowhead) can be localized in the lower, tympanic scala, suggesting this scala for implantation. In the registered 3D models (CT: gray, MRI: white), the fluid signal distribution within the inner ear can be tellingly demonstrated (D).

temporal bone. At any rate, it is likely that certain automated registration algorithms can be used quite soon to save time in the registration process by using them for a first, rough alignment.
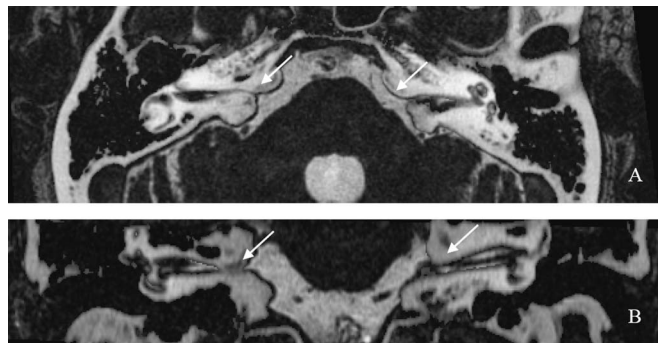
FIGURE 6. A patient suffering from myotonic dystrophy (Curschmann-Steinert) with hyperostotic lesions (arrows) around both IAC compressing their content. The registered and fused images (A: axial, B: coronal) showed to what extent the content of the IAC was dislocated and showed the expansion of the hyperostotic swellings. This improved surgical planning and helped the surgeon to avoid the IAC structures during surgery.

Clinical Benefit

Our results suggest that registration of CT and MRI of the temporal bone is most useful for assessing the relationship between bony and soft tissue structures.

In the registered images, the facial nerve can be seamlessly followed along its entire course. In malformations, this could improve diagnostic accuracy, because the facial nerve and its canal can be identified more reliably.

For tumor surgery within the IAC, accurate surgical planning is necessary. Almost all important surgical landmarks such as the IAC, facial nerve canal, inner ear, vestibular and cochlea aqueduct are all solely displayed in CT and the tumors are mostly solely displayed in MRI. Without registration, the surgeon relies on a rough assessment of the surgical approach by mentally integrating the information of both modalities. Registration of CT and MRI allows an assessment of the tumor extent relative to important surgical landmarks that need to be avoided during surgery. Especially the 3D imaging of the tumor together with important surgical landmarks can be beneficial for surgical planning and guiding during surgery. Furthermore, our method allows measurements to be taken within the registered dataset to objectively assess whether it is possible to reach the tumor through certain surgical approaches and therefore to assess the feasibility of various surgical approaches.

In cases of an extensively attenuated fluid signal within the cochlea, it is important to differentiate whether the signal arises from the vestibular or tympanic scala (Fig. 5), which results in alternative surgical approaches for cochlea electrode insertion. The electrode should be inserted in the scala that has the most fluid signal, because one can expect the best patency for implantation.[17,18] Since the fused images can give information about the fluid distribution not only relative to the bony labyrinth, but also relative to either scala, one can conclude which scala is the best to implant (a diagnosis that is hard to make from nonregistered and fused CT and MRI).

Another example that benefits from the registration of CT and MRI was the following case that was not included in the initial study: A patient (male, 53 years), suffering from myotonic dystrophy (Curschmann-Steinert), developed hyperostosis lesions around both IAC. A general hyperostosis potential is described in myotonic dystrophy,[19] but the coherency between myotonic dystrophy and hyperostosis around the IAC is not yet clear. The hyperostotic lesions compressed the content of both IAC and an impairment of the nerves and/or blood supply was assumed, causing the slow progredient, right accentuated, sensorineural hearing loss of the patient. The fused images (Fig. 6) facilitated surgical planning, because one could exactly assess the dislocation of IAC structures and the amount of bone that caused the dislocation. On the right-hand side, the IAC was almost totally occluded (Fig. 6B), resulting in the decision to ablate the hyperostosis on this side, expecting the biggest benefit for the patient. Furthermore, the surgeon knew beforehand where to expect the compressed IAC structures, which were dislocated to anterior–superior on the left and to more posterior–inferior on the right side.

CONCLUSION

In this study, co-registration and subsequent 3-dimensional visualization were evaluated for high-resolution CT and MRI of the temporal bone. An iterative, manual, retrospective, intrinsic and rigid approach for co-registration resulted in highly accurate and feasible multimodality images. We found that registered images are superior to conventional images for delineating the relationship between bony and soft tissue structures of the temporal bone. Excellent applications are the surgical planning for cochlea implantation and tumor surgery of the IAC, which can be further improved by 3D imaging of the structures from either modality together in 1 model. The only trade-off is the time need for the post

processing; therefore, we do suggest the registration and fusion of the temporal bone in special cases.

REFERENCES

1. Panigrahy A, Caruthers SD, Krejza J, et al. Registration of three-dimensional MR and CT studies of the cervical spine. *AJNR Am J Neuroradiol.* 2000;21:282–289.
2. Hill DL, Hawkes DJ, Gleeson MJ, et al. Accurate frameless registration of MR and CT images of the head: applications in planning surgery and radiation therapy. *Radiology.* 1994;191:447–454.
3. Maintz JB, Viergever MA. A survey of medical image registration. *Med Image Anal.* 1998;2:1–36.
4. Swartz JD. *Imaging of the Temporal Bone.* New York: Thieme; 1986.
5. Husstedt HW, Prokop M, Dietrich B, et al. Low-dose high-resolution CT of the petrous bone. *J Neuroradiol.* 2000;27:87–92.
6. Schmalbrock P. Comparison of three-dimensional fast spin echo and gradient echo sequences for high-resolution temporal bone imaging. *J Magn Reson Imaging.* 2000;12:814–825.
7. Gering DT, Nabavi A, Kikinis R, et al. An integrated visualization system for surgical planning and guidance using image fusion and an open MR. *J Magn Reson Imaging.* 2001;13:967–975.
8. Fitzpatrick JM, Hill DL, Shyr Y, et al. Visual assessment of the accuracy of retrospective registration of MR and CT images of the brain. *IEEE Trans Med Imaging.* 1998;17:571–585.
9. Hill DL, Batchelor PG, Holden M, et al. Medical image registration. *Phys Med Biol.* 2001;46:R1–45.
10. Muren C. The internal acoustic meatus. Anatomic variations and relations to other temporal bone structures. *Acta Radiol Diagn (Stockh).* 1986;27:505–512.
11. Gulya AJ, Steenerson RL. The scala vestibuli for cochlear implantation. An anatomic study. *Arch Otolaryngol Head Neck Surg.* 1996;122:130–132.
12. West JB, Fitzpatrick JM, Toms SA, et al. Fiducial point placement and the accuracy of point-based, rigid body registration. *Neurosurgery.* 2001;48:810–816; discussion 816–817.
13. Holden M, Hill DL, Denton ER, et al. Voxel similarity measures for 3-D serial MR brain image registration. *IEEE Trans Med Imaging.* 2000;19:94–102.
14. Mutic S, Dempsey JF, Bosch WR, et al. Multimodality image registration quality assurance for conformal three-dimensional treatment planning. *Int J Radiat Oncol Biol Phys.* 2001;51:255–260.
15. Wells WM 3rd, Viola P, Atsumi H, et al. Multi-modal volume registration by maximization of mutual information. *Med Image Anal.* 1996;1:35–51.
16. West J, Fitzpatrick JM, Wang MY, et al. Comparison and evaluation of retrospective intermodality brain image registration techniques. *J Comput Assist Tomogr.* 1997;21:554–566.
17. Hans P, Grant AJ, Laitt RD, et al. Comparison of three-dimensional visualization techniques for depicting the scala vestibuli and scala tympani of the cochlea by using high-resolution MR imaging. *AJNR Am J Neuroradiol.* 1999;20:1197–1206.
18. Ellul S, Shelton C, Davidson HC, et al. Preoperative cochlear implant imaging: is magnetic resonance imaging enough? *Am J Otol.* 2000;21:528–533.
19. Rodriguez JR, Castillo J, Leira R, et al. Bone anomalies in myotonic dystrophy. *Acta Neurol Scand.* 1991;83:360–363.